

# Kinetic Analysis of Heparin and Glucan Sulfates Binding to P-Selectin and Its Impact on the General Understanding of Selectin Inhibition<sup>†</sup>

Dirk Simonis,<sup>‡</sup> Juliane Fritzsche,<sup>‡</sup> Susanne Alban,<sup>§</sup> and Gerd Bendas<sup>\*,‡</sup>

Department of Pharmacy, Rheinische Friedrich Wilhelms University Bonn, An der Immenburg 4, 53121 Bonn, Germany, and  
Pharmaceutical Institute, Christian Albrechts University Kiel, Gutenbergstrasse 76, 24118 Kiel, Germany

Received November 14, 2006; Revised Manuscript Received March 16, 2007

**ABSTRACT:** P-Selectin, expressed on activated endothelial cells and platelets, is a high kinetic adhesion receptor involved in leukocyte rolling of the inflammatory response, or in tumor cell binding in the course of metastasis. Thus, P-selectin inhibition is a promising therapeutic target. The anti-inflammatory and anti-metastatic activities of heparin have partly been related to the inhibition of P-selectin binding. Here we apply a quartz crystal microbalance (QCM) biosensor to determine the kinetic constants of heparin and other sulfated polysaccharides binding to immobilized P-selectin. Binding kinetics of the derivatives were correlated with their inhibitory capacity in a P-selectin cell rolling assay. Three commercial heparins differ in cell rolling inhibition and display slightly different affinities ( $K_D$   $1.21 \times 10^{-6}$  M to  $5.86 \times 10^{-7}$  M). Inhibitory capacity appears to be mainly driven by a slow off-rate from the receptor ( $2.27 \times 10^{-3}$  s<sup>-1</sup> to  $1.23 \times 10^{-3}$  s<sup>-1</sup>). To correlate the impact of binding kinetics on inhibitory capacity structurally, we analyzed six semisynthetic glucan sulfates. They display different degrees of sulfation (DS), which has a strong influence on inhibitory activity. Kinetic data illustrate that the inhibitory capacity correlates excellently with the off-rate of these polysaccharides ( $R = 0.99$ ), while the association (on-rate) affects activity to a lesser extent. In general, the consideration of binding kinetics sheds new light on the mechanism of selectin inhibition. A much slower dissociation of the inhibitors from the receptor than the physiological ligands is key for inhibitory capacity. Structurally, highly charged compounds with a slow off-rate, such as heparin or glucan sulfates, appear as potent candidates for P-selectin inhibition.

The recruitment of leukocytes from the bloodstream into tissues is a functional basis for maintaining the cellular immune response. Leukocyte adhesion and emigration proceed in postcapillary venules of most organs in a cascade-like fashion (1). Selectins are a family of three carbohydrate-binding receptors on both endothelium (E- and P-selectin) and leukocytes (L-selectin) that initiate such adhesive events by mediating tethering and rolling of leukocytes along the vessel wall (2). Selectins are transmembrane glycoproteins that share a highly conserved N-terminal lectin domain (3).

The selectins are unique receptors in terms of their dynamic bond formation. Early experiments that focused on the transient unstressed binding events on substrates with low densities of P- or E-selectin suggested very rapid selectin–ligand bond dissociation rates (off-rates) of 1 s<sup>-1</sup> for P-selectin (4) and 0.5 s<sup>-1</sup> for E-selectin (5). Force spectroscopy experiments on single complexes of P-selectin interacting with PSGL-1 have been performed to determine rupture force dependence and bond lifetime (6). It was shown that P-selectin displays a catch bond behavior. Due to the catch–slip transitional bonds, the off-rates are a nonlinear biphasic function of applied force. These kinetic character-

istics were also found for L-selectin (7, 8) and explained as key mechanism to control adhesive events physiologically. Two recent studies reported on differences of unliganded versus liganded P- and L-selectin structures as basis for catch bond behavior (9, 10).

Surface plasmon resonance was used to detect the kinetic binding behavior of selectins. Nicholson et al. reported that soluble L-selectin binds to immobilized GlyCAM-1 with a very fast on-rate ( $k_{on} > 10^5$  M<sup>-1</sup> s<sup>-1</sup>)<sup>1</sup> and off-rate ( $k_{off} > 10$  s<sup>-1</sup>) and a moderate  $K_D$  of  $1.08 \times 10^{-4}$  M (11). P-Selectin that is especially important during the early phase of cell capturing displays an even faster association and higher binding affinity to immobilized PSGL-1 ( $K_D$   $3.0 \times 10^{-7}$  M,  $k_{off}$  1.4 s<sup>-1</sup>,  $k_{on}$   $4.4 \times 10^6$  M<sup>-1</sup> s<sup>-1</sup>) (12).

In general, the moderate binding affinity and rapid on- and off-rates of selectins were considered to be critically required for leukocyte rolling under shear force. The kinetic peculiarities of selectins complicate a potential inhibition of these adhesion receptors. The use of selectin-deficient animals has clearly proven that selectins are implicated in the development of pathological inflammations (13, 14), atherosclerosis, and cancer cell metastasis (15, 16). Therefore,

<sup>†</sup> This work was supported by the Deutsche Forschungsgemeinschaft, Graduiertenkolleg 677.

\* Corresponding author. E-mail: gendas@uni-bonn.de. Phone: +49 228 735250. Fax: +49 228 734692.

<sup>‡</sup> Rheinische Friedrich Wilhelms University Bonn.

<sup>§</sup> Christian Albrechts University Kiel.

<sup>1</sup> Abbreviations: DS, degree of sulfation;  $k_{on}$ , on-rate;  $k_{off}$ , off-rate;  $K_D$ , equilibrium dissociation constant; MW, molecular weight; QCM, quartz crystal microbalance; PhyS, phycarin sulfate; PSGL-1, P-selectin glycoprotein ligand-1; sLex, Sialyl Lewis x epitope ( $\alpha$ -Neu5Ac-(2→3)- $\beta$ -D-Gal-(1→4)-[ $\alpha$ -L-Fuc-(1→3)]- $\beta$ -D-GlcNAc-(1→R); UFH, unfractionated heparin.

the blocking of selectins has attracted much attention as a promising strategy for therapeutic interventions.

The minimal binding structure recognized by all selectins, the tetrasaccharide sLex (17), displays certain anti-inflammatory activity (18–21). It was regarded as lead structure to design sLex mimetics, but the very low binding affinities of sLex ( $K_D$   $0.1\text{--}5.0 \times 10^{-3}$  M) (22) could not be improved fundamentally by structural modifications. Presently, only few compounds are investigated in advanced preclinical or clinical trials (23).

An impact of binding kinetics on inhibitory potency has not been considered so far. A recent study by Beauharnois et al. reported on the binding kinetics of the drug candidate TBC 1269 (24). The rapid off-rate of TBC 1269 from P-selectin of  $>3\text{ s}^{-1}$  is similar to that of sLex and the physiological ligands. Whether the rapid off-rate is a limiting factor for the inhibitory potency of sLex-based small molecules cannot be answered from the present data.

Since electrostatic interactions dominantly contribute to P-selectin ligand binding (25), interest focused on highly charged, higher molecular weight (MW) structures as potential inhibitors. This is in line with earlier studies showing that sulfated polysaccharides, such as fucoidan or heparin, bind to P-selectin (26, 27).

Heparin belongs to the group of glycosaminoglycans and is a complex, highly sulfated polysaccharide mixture with a MW between 3000 and 30 000. Heparins, i.e., unfractionated heparins (UFH) and various low molecular heparins, have been the antithrombotic drug of choice for more than 65 years. The anti-inflammatory and antimetastatic effects of heparin are assumed to be at least partly due to their P-selectin blocking capacity (15, 28). Initial studies indicated that heparins can act as ligands for P- and L-selectin and interfere with sLex-related structures (26, 27, 29, 30). Structure–activity relationships show that the selectin-binding properties of heparins are independent of the antithrombin binding site and can be varied by structural modifications (30–34). However, the fact that heparins represent highly complex molecule mixtures that may show batch-to-batch variability complicates the deduction of clear structure–activity relationships. We recently applied a series of well-defined glucan sulfates in a cell rolling assay (35, 36) to establish the structural requirements for P-selectin inhibitory capacity of sulfated polysaccharides.

Wang et al. investigated the binding kinetics of heparin to P-selectin using surface plasmon resonance (37). They measured a  $K_D$  of  $1.15 \times 10^{-7}$  M that supports the experimentally found potency of heparin. They suggest that the slow off-rate ( $3.15 \times 10^{-3}\text{ s}^{-1}$ ) indicates that heparan sulfate containing cells adhere firmly, in contrast to PSGL-1 containing cells that show a rolling movement.

In the present study, we emphasize the interest on heparin and glucan sulfates as P-selectin inhibitors. To clarify the role of binding kinetics for inhibitory potency, we determined the kinetics of heparin and glucan sulfates binding to P-selectin using quartz crystal microbalance (QCM) and correlated the data with a cell rolling inhibition assay.

QCM is the most prominent mass-sensitive biosensor technique. It is based on the piezoelectric properties of quartz crystals that enable an electrical excitation and oscillation measurement of a thin quartz sensor. Since the resonance frequency of these oscillations correlates with the mass load

on its surface (38), changes in mass can be detected in real time by monitoring the frequency shifts. The use of flow chamber equipment allows the calculation of kinetic binding constants of ligands to surface-immobilized receptors. Although the QCM method has already been established for several analytical approaches (39–41), this technique has not yet been applied in selectin or heparin research.

We provide the first direct measurement of the affinity and kinetics of heparin and other sulfated polysaccharides to P-selectin using QCM. The data give a general insight into the selectin inhibitor research. The direct correlation of binding kinetics with cell rolling inhibition emphasizes the role of a slow off-rate for inhibitory capacity. Highly charged polysaccharides display much slower dissociation rates than natural ligands and, thus, appear to be excellent inhibitors.

## EXPERIMENTAL PROCEDURES

**Materials.** Recombinant human P-selectin–Fc chimera and recombinant human PSGL-1–Fc chimera (rPSGL-1) were purchased from R&D Systems, Wiesbaden, Germany. Purified anti-human CD62P and purified mouse IgG $_{1\kappa}$  were from Becton Dickinson GmbH, Heidelberg, Germany. Bovine serum albumin (BSA) and cyanuric chloride were purchased from Sigma, Deisenhofen, Germany. 6-Mercaptohexan-1-ol was purchased from Fluka, Neu-Ulm, Germany, and chloroform was from Riedel de-Haen, Seelze, Germany. All salts and buffers were of analytical grade.

**Sulfated Polysaccharides.** Low molecular weight fucoidan (from brown seaweed; average MW 8.2 kDa) was purchased from Kraeber, Ellerbek, Germany.

Three UFH products were included in the study: Calciparin (Sanofi-Synthelabo GmbH, Berlin, Germany, Ch.B. 540234, 5000 IU, 0.2 mL), Liquemin N 5,000 (Hoffman-La-Roche AG, Grenzach-Wyhlen, Germany, Ch.-B. F002611, 5000 IU, 0.5 mL), and Heparin-Natrium-5,000-ratiopharm (Ratiopharm GmbH, Ulm, Germany; Ch.-B. F21916, 5000 IU, 0.2 mL). The concentration of Calciparin was assumed as declared (5000 IU/0.2 mL). According to the analytical certificate, the concentration of the employed Liquemin N was 10 497 IU/mL, i.e., 105.0% of the declared concentration, whereas that of Heparin-ratiopharm was 24 075 IU/mL, i.e., 96.3%.

Semisynthetic linear glucan sulfates were produced by sulfation of the natural polysaccharide phycarin (PhyS) (Goemar Laboratories, St. Malo, France), a  $\beta$ -1,3 glucan (degree of polymerization 23–25) with  $\text{SO}_3$ /pyridine in dimethylformamide as described (42, 43). The degree of sulfation (DS, sulfate groups per glucose unit) of the phycarin sulfates (PhyS) was determined by ion chromatography on a HPLC system, and their molecular weight ( $\text{MW}_{\text{HD}}$ ), i.e., their hydrodynamic volume, by gel permeation chromatography using neutral derivatives of defined MW as standards. The PhyS have an average  $\text{MW}_{\text{HD}}$  of about 18–19 kDa that corresponds to an average MW of 10 kDa (as confirmed by ESI-MS). The sulfation pattern of the glucan sulfates was established by methylation–ethylation analysis with subsequent gas–liquid chromatography–mass spectrometry of the resulting partially methylated, ethylated alditol acetates (44).

**Preparation of the Quartz Crystal Surface.** Quartz crystals were cleaned using piranha solution ( $\text{H}_2\text{O}_2$  concentrated/-

H<sub>2</sub>SO<sub>4</sub> concentrated 1/3) and subsequently rinsed with demineralized water. After repeating this procedure three times, the quartz crystals were rinsed with ethanol (abs.) and dried under a stream of synthetic air. The cleaned quartz crystals were added to a 1 mM chloroform solution of 6-mercaptohexan-1-ol for about 12 h at rt to form a thiol-functionalized monolayer. After rinsing the quartz crystals briefly with ethanol and drying them under a stream of synthetic air, the quartz crystals were put into a chloroform solution of cyanuric chloride (1% mass/volume) for 2 h at rt, again followed by ethanol washing and drying. The cyanuric chloride acts as a reactive linker onto the immobilized 6-mercaptohexan-1-ol for coupling the P-selectin–Fc chimera. A solution of 20  $\mu$ L P-selectin–Fc chimera in PBS (0.2  $\mu$ g/ $\mu$ L) and 20  $\mu$ L of borate buffer (pH 8.8) was put on the upper gold surface of the quartz sensors. After 2 h at rt, the quartz crystals were rinsed once again with demineralized water and dried under a stream of air. For blank experiments, a solution of 20  $\mu$ L of BSA (20% mass/volume) in PBS was used instead of P-selectin–Fc chimera.

**QCM Measurements.** QCM measurements were performed with a LiquiLab21 quartz crystal microbalance (ifak e.V., Barleben, Germany). Measurement chambers were made of polycarbonate. They had a chamber volume of 100  $\mu$ L. A peristaltic pump assured both flow conditions and the transport of the substance solutions to the quartz crystal surface. AT-cut quartz crystals with 10 MHz resonance frequency (14 mm diameter) were supplied by ifak e.V. The quartz crystals were inserted into the measurement chambers. PBS buffer with Ca<sup>2+</sup> (1 mM) and Mg<sup>2+</sup> (1 mM) was used for the flow. The experiments were performed under a volume flow rate of 270  $\mu$ L min<sup>-1</sup>, which roughly corresponds to a shear rate of 5 s<sup>-1</sup>. The quartz crystals were equilibrated under flow conditions for 30 min to reach a constant resonance frequency. The indicated concentrations of polysaccharides, PSGL-1, or antibodies were added under constant flow conditions. The change of frequency was monitored in real time using appropriate software.

**Calculation of the Kinetic Data.** The kinetic data were calculated from the monitored frequency curves. We checked a pseudo-first-order kinetic behavior according to the findings of Minunni et al. (45). For this task we plotted  $df/dt$  vs the corresponding frequency changes in the descending part of the curve applying different concentrations of the test compounds. We obtained straight lines for each experiment and therefore assumed pseudo-first-order kinetics of P-selectin binding. The on-rate was calculated from the descending part of the curve according to eq 1.  $\Delta f$  is the measured frequency change at the time point  $t$ ,  $[A]$  is the concentration of the injected compounds, and  $f_{\max}$  is the maximum frequency change of the completely loaded quartz crystal.  $t_0$  is the time when the decrease of the frequency begins.

$$\Delta f = -\frac{k_{\text{on}}[A] + f_{\max}}{k_{\text{on}}[A] + k_{\text{off}}} (1 - e^{-k_{\text{on}}[A] + k_{\text{off}}(t-t_0)}) \quad (1)$$

After the maximum change of frequency was achieved, rinsing with PBS led to a frequency increase that permitted the calculation of the off-rate ( $k_{\text{off}}$ ), according to eq 2, where  $f_0$  is the frequency value at  $t_0$ , where  $t_0$  is the time when the

increase of frequency begins.  $f$  is the frequency value at the point in time  $t$ . The  $k_{\text{off}}/k_{\text{on}}$  ratio yields the equilibrium dissociation constant  $K_D$  (eq 3).

$$\Delta f = \Delta f_0 e^{-k_{\text{off}}(t-t_0)} \quad (2)$$

$$K_D = \frac{k_{\text{off}}}{k_{\text{on}}} \quad (3)$$

**Cell Cultivation.** U937 cells, a human monocytic cell line expressing PSGL-1, were cultivated at 37 °C and 5% CO<sub>2</sub> in RPMI 1640 medium containing 10% fetal calf serum and 1% penicillin–streptomycin solution (Sigma, Deisenhofen, Germany). PSGL-1 expression was routinely analyzed by FACS. The cells were used for the rolling experiments within 4 h after separation, centrifugation, and suspension into a serum free medium.

**Laminar Flow Experiments.** The cell rolling experiments and microscopic detection of inhibitory capacities were performed in a plate flow chamber assay as described in detail (36). For the flow experiments,  $1 \times 10^6$  U937 cells in 100  $\mu$ L of pure medium (control experiment) or containing the inhibitors (corresponding to 50  $\mu$ g/mL after dynamic dilution in the flow chamber) were injected into the streaming medium and analyzed immediately. Cell rolling or adhesion onto immobilized P-selectin chimera was monitored for 10 s capturing 25 frames per second with a CSC 795 camera using a long distance objective of 20 $\times$  magnification. The video sequences were saved and analyzed by application of appropriate software (Imagoquant Multitrack-AVI-2, Medi-quant, Halle, Germany) resulting in detailed and automated analysis of the experimental data. All cells (about 150) per image were analyzed for the evaluations. Inhibition of cell rolling is expressed as cell number at  $t = 4$  s, divided by the number on the start image ( $t = 0$  s). The results were illustrated as percentage adhesion related to the control experiment.

**Coagulation Assays.** The coagulation assays were performed using citrated human platelet depleted pool plasma prepared according to the guidelines for preparing citrated plasma for hemostaseological analyses and stored at -70 °C until testing. The clotting times were measured with the Kugelcoagulometer KC 10 (Amelung, Lemgo, Germany). To determine the concentration dependent anticoagulant activity of heparin, 90  $\mu$ L of plasma, freshly thawed at 37 °C, was mixed with 10  $\mu$ L of heparin dilution (0.9% mass/volume in NaCl, or 10  $\mu$ L 0.9% mass/volume NaCl for the baseline coagulation time, respectively). From each heparin, two dilution series were prepared by two persons.

At the activated partial thromboplastin time (APTT), the supplemented plasma was incubated for 60 s at 37 °C. Then, 100  $\mu$ L of Pathromtin SL (Dade Behring, Bad Schwalbach, Germany) was added. After 120 s incubation at 37 °C, the coagulation was initiated by 100  $\mu$ L of 0.025 M CaCl<sub>2</sub> solution preheated at 37 °C.

At the thrombin time, the supplemented plasma was incubated for 60 s at 37 °C. Then, the coagulation was initiated by 200  $\mu$ L of Test-Thrombin-Reagenz (bovine) (Behringwerke, Marburg, Germany) preheated to 37 °C. Each sample of the two dilution series of each heparin was measured between 2 and 6 times. Two repetitions of all the determinations resulted in day to day variations of less than 5%.



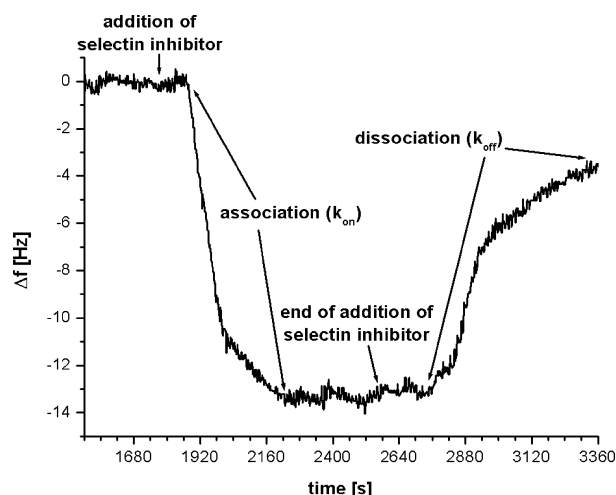


FIGURE 1: Representative example of a frequency course illustrating a kinetic binding process detected by the QCM biosensor.

**Statistical Analysis.** Data are represented as means of at least three identical and independent experiments  $\pm$  standard deviation (SD). Statistical comparisons were performed with the unpaired Student's *t*-test.

## RESULTS

**Application of the Biosensor System for P-Selectin Binding Kinetics.** QCM is a mass sensitive biosensor technique. The binding of compounds from the flowing medium onto the functionalized quartz surface can be observed with high reproducibility in real time following the frequency shifts as illustrated in Figure 1.

After equilibrating the resonance frequency under flow of pure medium, binding leads to a significant decrease in frequency to a minimum that represents the equilibrium of binding. Replacement of the medium by pure buffer illustrates the dissociation of bound compounds, manifested in a certain frequency increase. The course of frequency change allows the calculation of the kinetic binding constants by an exponential curve fitting in the indicated areas according to eqs 1 to 3. In the area in between, equilibrated association and dissociation can be assumed due to the experimental setup.

In order to focus on kinetic binding behavior, we did not need to quantify absolute changes in frequency, but considered frequency slopes only. Therefore, the amount of immobilized P-selectin at the quartz surface appeared to be a more important factor influencing the experiments than the concentration of the inhibitors. Consequently, a certain amount of inhibitor within a concentration range covering a 1:1 (inhibitor:selectin) binding ratio seemed sufficient, as long as it created significant frequency changes.

We chose fucoidan as a standard compound for P-selectin binding. The fucoidan used has a comparable MW to unfractionated heparin (UFH) and was shown to bind P-selectin strongly (36). To optimize the P-selectin immobilization, the amount of P-selectin-Fc chimera for reaction on the effective quartz surface was modified from 1  $\mu$ g to 5  $\mu$ g, keeping a constant concentration of  $4 \times 10^{-6}$  M fucoidan solution (corresponding to 33  $\mu$ g/mL). The absolute frequency changes for the interaction are illustrated in Figure 2. The immobilization of 4  $\mu$ g of P-selectin-Fc chimera represents the saturation of the binding reaction.

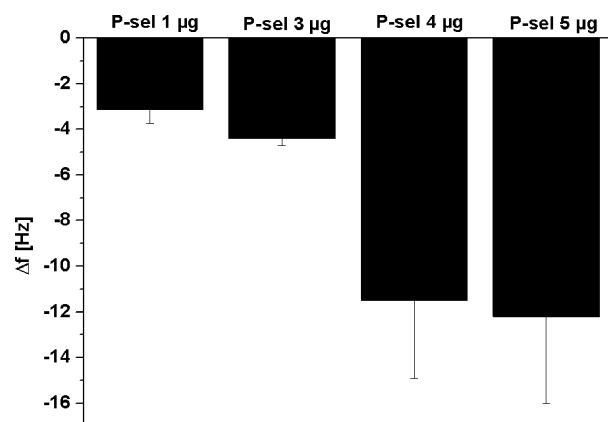


FIGURE 2: Optimization of quartz sensor biofunctionalization. Absolute frequency changes (means,  $\pm$  SD,  $n = 3$ ) induced by the interaction with a  $4 \times 10^{-6}$  M fucoidan solution with respect to four different amounts of immobilized P-selectin-Fc chimera.

As we were able to obtain similar relations using other concentrations of fucoidan (data not shown), the immobilization of 4  $\mu$ g of P-selectin was chosen for the following experiments.

In order to confirm both functionality of the assay and binding specificity of immobilized P-selectin-Fc chimera, we analyzed the binding characteristics of an anti P-selectin antibody and rPSGL-1-Fc chimera. Kinetic analysis of the antibody binding course displayed the typical affinity of a specific IgG molecule, binding the antigen in the high picomolar range. This affinity results from a high on-rate and a prominently slow off-rate. Since a binding could not be observed using a control IgG, the functionality of the assay was confirmed.

In comparison to the antibody, the rPSGL-1 has a lower affinity in the high nanomolar range that is mainly induced by the much faster dissociation. Although the published data refer to the natural PSGL-1 in dimeric form, the affinity of the recombinant monomeric protein in our study is in a comparable range ( $5.59 \times 10^{-7}$  M vs  $3.0 \times 10^{-7}$  M) (46). Although no kinetic data were published for rPSGL-1 that would allow a validation of our assay, the higher affinity of the dimer vs monomer is plausible and was recently shown in binding force experiments (6). However, the on- and off-rate of the rPSGL-1 differ from the data found for natural PSGL-1 by a slower association and slower dissociation tendency. This might be related to structural differences, such as monomer vs dimer, the presence of the Fc moiety, or the experimental conditions of the assays used (immobilized P-selectin vs immobilized PSGL-1). Nevertheless, these data confirm that the biosensor is functionally active, and P-selectin is accessible for specific binding reactions.

**Binding Kinetics of Heparins on P-Selectin.** In the established QCM system, we first examined the binding kinetics of UFH. Due to the natural variability of their structural composition, the biological activities may vary between different UFH preparations. In the clinical application as antithrombotics, UFH is therefore not dosed in gravimetric concentrations, but in International Units (IU) reflecting their respective *in vitro* anticoagulant activity. However, the anticoagulant activity was shown to be uncorrelated to their further biological activities, especially with their P-selectin antagonizing effect (47). Consequently,

Table 1: Kinetic Constants of rPSGL-1 and Anti-P-Sel mAb Binding to Immobilized P-Selectin, Calculated from the Frequency Slopes of the QCM Measurements (Means,  $\pm$  SD,  $n \geq 3$ )

	$K_D$ [M]	$k_{on}$ [ $M^{-1} s^{-1}$ ]	$k_{off}$ [ $s^{-1}$ ]
rPSGL-1	$5.59 \times 10^{-7}$ $\pm 1.07 \times 10^{-8}$	$2.61 \times 10^4$ $\pm 1.65 \times 10^3$	$1.20 \times 10^{-2}$ $\pm 2.36 \times 10^{-3}$
anti P-Sel mAb	$1.98 \times 10^{-10}$ $\pm 1.34 \times 10^{-12}$	$2.02 \times 10^5$ $\pm 1938$	$4.00 \times 10^{-5}$ $\pm 5.45 \times 10^{-7}$

identical anticoagulant doses of different UFH preparations may exhibit different P-selectin inhibitory activities and may differ in their overall therapeutic efficacy. In a previous study, we accordingly found slight differences between the P-selectin inhibitory potency of two UFH preparations, Liquemin N and Heparin-ratiopharm, in a cell rolling assay (36).

In order to investigate whether these natural variabilities are reflected in binding kinetics, we selected three commercially available UFHs for the present study, the two mentioned products and Calciparin.

First, we verified that identical IU/mL concentrations have the same anticoagulant effects. Therefore, we detected both the APTT and thrombin time of the products and correlated them with the declared or indicated activity (data not shown). Finally, we could conclude that identical IU/mL of the UFH products used were confirmed to exhibit identical anticoagulant activities.

In our previous investigations (36), Heparin-ratiopharm showed a slightly higher inhibitory capacity for P-selectin-mediated cell rolling than Liquemin N. The effects in this assay are, however, concentration-dependent so that any conclusions about different activities generally depend on the concentrations used for comparison. In this respect, the QCM technique has the clear advantage that the obtained kinetic data are independent of the exact concentration, as long as one can ensure a 1:1 binding stoichiometry according to a pseudo-first-order kinetic behavior (45). In order to select an optimal concentration for detection, we analyzed four different concentrations, ranging from  $1.28 \times 10^{-6}$  M (17  $\mu$ g/mL) to  $1.28 \times 10^{-5}$  M (170  $\mu$ g/mL) with respect to the kinetic binding behavior. Although we were able to obtain similar  $k_{off}$  values for all four concentrations, higher amounts than  $5.12 \times 10^{-5}$  M and 67  $\mu$ g/mL, respectively, tended to lower the  $k_{on}$ . The lower  $k_{on}$  reflects that not all heparin molecules adequately bind to the immobilized selectin. But as it is considered by eq 1, the calculation of  $k_{on}$  cannot be applied properly. Based on these findings we choose  $2.56 \times 10^{-6}$  M (33  $\mu$ g/mL) for further heparin investigations. The kinetic binding data obtained for the UFHs are summarized in Table 2.

The  $K_D$  values from  $1.21 \times 10^{-6}$  M to  $5.86 \times 10^{-7}$  M indicate that heparin binds P-selectin with high affinity. Although the data illustrate that the three heparin products are comparable in binding, Calciparin differs remarkably from the others, as it has the lowest association tendency and a faster dissociation. Heparin-ratiopharm, which had a higher inhibitory capacity for P-selectin-mediated cell rolling than Liquemin N in our previous investigations (36), displays slightly higher affinity. Although Heparin-ratiopharm has a lower on-rate than Liquemin N, the slower off-rate ( $k_{off}$   $1.23 \times 10^{-3} s^{-1}$  vs  $1.96 \times 10^{-3} s^{-1}$ ) appears to contribute dominantly to affinity and inhibitory activity.

Table 2: Kinetic Constants of Calciparin, Liquemin N, and Heparin-ratiopharm Binding to Immobilized P-Selectin, Calculated from the Frequency Slopes of the QCM Measurements (Means,  $\pm$  SD,  $n \geq 3$ )

	$K_D$ [M]	$k_{on}$ [ $M^{-1} s^{-1}$ ]	$k_{off}$ [ $s^{-1}$ ]
Calciparin	$1.21 \times 10^{-6}$ $\pm 1.42 \times 10^{-7}$	$1.91 \times 10^3$ $\pm 337$	$2.27 \times 10^{-3}$ $\pm 1.66 \times 10^{-4}$
Liquemin N	$6.07 \times 10^{-7}$ $\pm 1.34 \times 10^{-7}$	$3.27 \times 10^3$ $\pm 561$	$1.96 \times 10^{-3}$ $\pm 1.62 \times 10^{-4}$
Heparin-ratiopharm	$5.86 \times 10^{-7}$ $\pm 2.64 \times 10^{-7}$	$2.31 \times 10^3$ $\pm 741$	$1.23 \times 10^{-3}$ $\pm 2.70 \times 10^{-4}$

These data indicate that the heparin products, although identical in their anticoagulant activity, show differences in P-selectin binding.

*P-Selectin Binding Kinetics of Chemically Defined Glucan Sulfates.* The heparin data give indications that the P-selectin inhibition depends on the binding kinetics. However, the data of the three heparins allow for detailed discussions neither on the impact of on-rate and off-rate on the inhibition nor on their dependency on structure. The mean DS of all the UFHs is 1.1 per monosaccharide (1.0–1.2), and, by definition, the degree of carboxylation is 0.5 per monosaccharide. The absence of differences in the charge density between the different UFH preparations suggests that other structural parameters are responsible for the different kinetics.

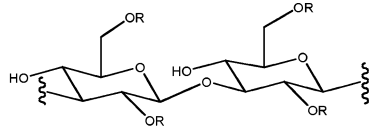
In order to derive clear correlations between structures, binding kinetics, and inhibitory capacity, we applied a series of chemically defined semisynthetic glucan sulfates, as introduced in Table 3. The indicated members of the phycarin sulfate (PhyS) family consist of an identical  $\beta$ -1,3 linked glucan backbone of comparable size (10 kDa), but differ in charge density, as represented by their degree of sulfation (DS). The different PhyS were applied for the kinetic binding detection at a similar amount as the UFHs (33  $\mu$ g/mL,  $2.78 \times 10^{-6}$  M, respectively). No interaction of the noncharged phycarin (PhyS 1) with P-selectin could be observed. This confirms the essential role of charge for P-selectin interaction. The other glucan sulfates (PhyS 2 to PhyS 6) displayed a distinct binding ability to P-selectin. The resulting binding kinetic constants are summarized in Table 3.

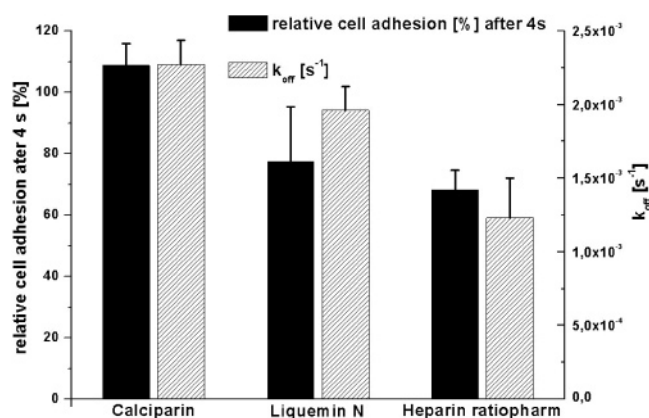
When considering the binding affinity of the PhyS, a clear dependency on the charge density becomes evident. While the low charged PhyS 2 (DS 0.75) has an about 10-fold lower affinity than the heparins, PhyS 3 is roughly comparable to heparin, while PhyS 4 to Phys 6 exceed the heparin affinities strictly.

To evaluate the impact of the on-rate on the affinity, the data of PhyS 2 to PhyS 6 were considered with respect to their structures. In general, one can assume that a charge increase should lead to higher association rates. This tendency is evident in Table 3. The significantly lower on-rate of PhyS 5 compared to the very rapid association of PhyS 6 cannot be explained properly.

In order to derive the impact of the off-rate on binding affinity and inhibition, we first considered the heparin data. It is evident that the slightly more active inhibitor (Heparin-ratiopharm) has a marginally slower off-rate compared to Liquemin N. To relate the off-rates to inhibitory capacity, we also detected the cell rolling inhibition of Calciparin and

Table 3: Backbone Structure and Degree of Sulfation (DS) of PhyS 1 to PhyS 6 and Their Kinetic Constants of Binding to Immobilized P-Selectin (Means,  $\pm$  SD,  $n \geq 3$ ), as Detected by QCM

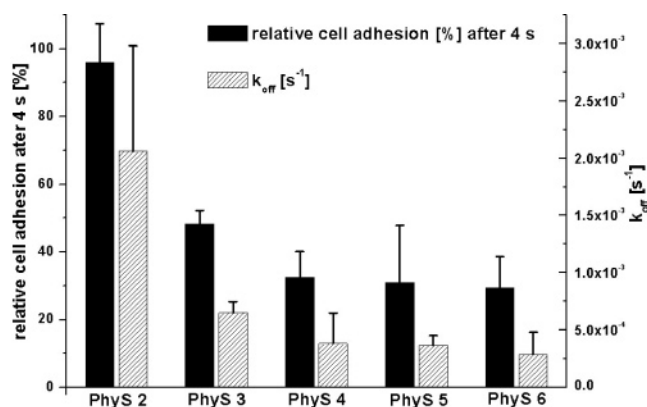
 R=H/SO <sub>3</sub> Na		degree of sulfation (DS)	$K_D$ [M]	$k_{on}$ [M <sup>-1</sup> s <sup>-1</sup> ]	$k_{off}$ [s <sup>-1</sup> ]
PhyS 1		0.00	not detectable		
PhyS 2		0.75	$9.16 \times 10^{-6}$ $\pm 2.68 \times 10^{-6}$	522 $\pm 176$	$2.06 \times 10^{-3}$ $\pm 9.20 \times 10^{-4}$
PhyS 3		1.48	$5.01 \times 10^{-7}$ $\pm 2.78 \times 10^{-7}$	$1.72 \times 10^3$ $\pm 1.11 \times 10^3$	$6.50 \times 10^{-4}$ $\pm 9.84 \times 10^{-5}$
PhyS 4		1.80	$1.59 \times 10^{-7}$ $\pm 9.10 \times 10^{-8}$	$2.47 \times 10^3$ $\pm 911$	$3.83 \times 10^{-4}$ $\pm 2.66 \times 10^{-4}$
PhyS 5		2.21	$1.70 \times 10^{-7}$ $\pm 4.03 \times 10^{-8}$	$2.16 \times 10^3$ $\pm 39$	$3.67 \times 10^{-4}$ $\pm 8.50 \times 10^{-5}$
PhyS 6		2.80	$4.39 \times 10^{-8}$ $\pm 2.54 \times 10^{-8}$	$6.64 \times 10^3$ $\pm 1.78 \times 10^3$	$2.87 \times 10^{-4}$ $\pm 1.95 \times 10^{-4}$

FIGURE 3: Comparison of the inhibitory capacity in a P-selectin induced cell rolling assay after 4 s (left ordinate) and the off-rates of Calciparin, Liquemin, and Heparin-ratiopharm as detected by QCM (right ordinate): The number of adhering and rolling U937 cells is expressed as a percentage of the blank (means,  $\pm$  SD values,  $n \geq 3$ ).

illustrated the dependency in Figure 3. Inhibitory effects were selected at a 4 s time point in an activity vs time slope, since this represents the saturation of activity.

Calciparin displayed no inhibitory activity in the cell rolling assay. Although this is surprising, and should more be related to the sensitive restrictions of the cell rolling assay than to a binding inability of Calciparin, this finding fits well to the 2-fold higher off-rate compared to Heparin-ratiopharm. Although the data set of only three different products does not allow a mathematical correlation, the off-rate is obviously a decisive factor controlling the inhibitory characteristics of the derivatives.

This hypothesis is strongly supported by considering the off-rates of the PhyS in Figure 4 (hatched bars, right ordinate). An increase in charge from Phys 2 to Phys 6 leads to a nonlinear decrease in off-rate, which implies that electrostatic interactions dominate the intensity of receptor occupation. In order to correlate the receptor binding with the inhibitory efficiency of the compounds, the inhibition data of the PhyS, obtained from the cell rolling assay, were included in Figure 4 (dark bars, left ordinate). An excellent correlation between the inhibitory capacity of the compounds and the off-rate becomes evident ( $R = 0.99$ ).

FIGURE 4: Comparison of the inhibitory capacity of PhyS 2 to PhyS 6 in a P-selectin induced cell rolling assay after 4 s (left ordinate) and the off-rate as detected by QCM (right ordinate): The number of adhering and rolling U937 cells is expressed as a percentage of the blank (means,  $\pm$  SD values,  $n \geq 3$ ). Both experimental lines correlate excellently ( $R = 0.99$ ).

## DISCUSSION

Although the inhibition of selectin binding function has attracted tremendous interest to interfere therapeutically with various pathological situations, hardly any reports on kinetic binding data of inhibitors exist. Therefore it cannot be evaluated if the rapid binding kinetics of the selectins are responsible for the nonsatisfying situation and complications in the selectin inhibitor search.

In the present study we applied a QCM biosensor to quantify the kinetic binding of heparins and other sulfated polysaccharides to surface-immobilized P-selectin. To investigate the relevance of these intrinsic binding characteristics for the functional role in cell binding, we also detected the inhibitory activity of these derivatives in a P-selectin-mediated cell rolling assay. To our knowledge, this is the first time that the inhibitory capacity is correlated with binding kinetics for a series of compounds to give a general insight into the mechanisms of selectin inhibition.

We could illustrate that heparin binds to P-selectin with strong binding affinity. This confirms several approaches that applied heparin as an attractive P-selectin inhibitor for anti-inflammatory and antimetastatic reasons (16, 28, 48). However, the three heparin products displayed deviations in



affinity ( $5.80 \times 10^{-7}$  M,  $6.07 \times 10^{-7}$  M, and  $1.21 \times 10^{-6}$  M) that reflect the structural variations of the heparin products. Nevertheless, the heparin affinity is consistent with the recent findings of Wang et al. (37), the only published kinetic data of a heparin binding to P-selectin. They used heparin-conjugated BSA for immobilization on the chip sensor surface and analyzed the interaction with soluble P-selectin by surface plasmon resonance. While the affinity of  $1.15 \times 10^{-7}$  M and the off-rate of about  $3.15 \times 10^{-3} \text{ s}^{-1}$  described by Wang et al. is close to our findings, they found a higher on-rate. This variation might be explained by differences in the experimental setup, i.e., the immobilization of heparin by Wang et al. versus the use of immobilized selectin in our approach.

Wang et al. interpreted these kinetic findings with respect to cell adhesion phenomena. They postulated that the moderately fast association of heparin and the much slower off-rate in relation to the physiological ligand PSGL-1 can explain that tumor cells expressing heparan sulfates as P-selectin ligands are not able to roll along the endothelium, such as PSGL-1 expressing cells. We try to interpret the heparin binding kinetics with respect to consequences for the selectin inhibitor search. A fast on-rate that is much higher for the natural PSGL-1 compared to heparin appears to be an essential prerequisite for all binding processes to selectins under shear conditions. However, exceeding a certain threshold level of association tendency, graduations in the on-rate appear to have a lesser impact on the overall selectin binding characteristics. The off-rate directly controls the duration of the receptor occupation. Taking the off-rate of PSGL-1 into consideration, heparin is able to occupy the receptor 1000-fold longer, which appears as a dominant contribution to the binding process, and therefore important for inhibitory activity.

Considering the structures, a slow off-rate might be induced by the intensity of the charge interactions. The polysaccharide nature and the charge density of heparin appear to be predestined for inducing a slow dissociation. However, extended discussions on a structural impact on binding were limited by the fact that heparin is a complex mixture of sulfated polysaccharides of animal origin that leads to product variability. Identical anticoagulative activity of the three products in our study was shown to be not indicative for other biological functions, such as selectin binding. The three UFHs differ in the off-rate from  $2.27 \times 10^{-3} \text{ s}^{-1}$  to  $1.23 \times 10^{-3} \text{ s}^{-1}$ , and interestingly, these differences in the off-rate clearly reflect the graduation in the P-selectin inhibitory capacity found in the cell rolling assay. This trend is not evident in the on-rates as Liquemin N with the lowest inhibitory capacity has the highest on-rate. This has also an influence on the  $K_D$  values that readily show the trend of the inhibition. Although these findings advise a role of the off-rates for the binding ability and inhibitory capacity, the deviations of the products do not allow general conclusions.

The application of the PhyS derivatives clarifies whether the dependence of inhibitory capacity and the off-rate is an arbitrary finding or a general factor for inhibition. Detecting their binding kinetics to P-selectin as well as their P-selectin inhibition gives a deeper insight into (i) the dependency of binding kinetics on a gradual change in the molecular charge

density and (ii) a general correlation of binding kinetics and inhibition.

The importance of a charge increase on binding affinity could clearly be derived, considering the  $K_D$  in Table 3. A charge increase induces higher binding affinities. The derivatives with a DS  $\geq 1.8$  exceed the affinity of the heparins. PhyS 6 displays an outstanding affinity with a  $K_D$  of  $4.39 \times 10^{-8}$  M that has not been described so far for an artificial compound binding P-selectin. However, the impact of the on- and the off-rate on this affinity increase is different. An increase in on-rate with increased charge density is evident, but does not show a correlation, as the relation of PhyS 4 (DS 1.80) to PhyS 5 (DS 2.21) and the rapid increase to PhyS 6 (DS 2.80) underscores. In contrast, the off-rate follows the increased affinity by charge density much better.

To investigate the impact of these kinetic findings on inhibitory efficiency, we compared the reduction in cell binding by PhyS 2 to PhyS 6 in the cell rolling assay with the kinetic parameters. The slope in cell rolling inhibition that is illustrated in Figure 4 by the dark bars is barely correlated with the on-rate ( $R = 0.67$ ). In contrast, there is an excellent correlation with the off-rate ( $R = 0.99$ ). This confirms the hypothesis on the importance of the off-rate for inhibition, that we postulated from the heparin data.

More importantly, these data allow for the first time the derivation of a general interpretation on selectin inhibition and the mechanisms and prerequisites for potential selectin inhibitors. While cell binding or cell rolling assays represent a functional end point in diminishing the cell binding by certain inhibitors, our kinetic interpretations give a much deeper mechanistic insight. A certain fast on-rate that does not necessarily have to be faster than the on-rate of the physiological selectin ligands appears as the basis for selectin binding. Exceeding a threshold in binding rapidity, the on-rate has only a minor effect on the general affinity. In contrast, the receptor occupation by a slowly dissociating compound controls the binding intensity and turns out to be key for inhibitors. We were able to show that a 1000-fold lower off-rate of heparin and related polysaccharides compared to the physiological ligands or small molecule inhibitors is the functional background for their excellent inhibitory capacity.

Overall, these findings give general indications for the design and search of selectin inhibitors. Kinetic parameters, e.g., a slow off-rate, must ultimately be considered. Since we were able to show that the binding kinetics are controlled by certain structural parameters, i.e., charge density, highly charged polysaccharides appear as prospective inhibitory compounds.

## ACKNOWLEDGMENT

The authors would like to thank Felix Momsen for reading the manuscript critically.

## REFERENCES

1. Steeber, D. A., and Tedder, T. F. (2000) Adhesion molecule cascades direct lymphocyte recirculation and leukocyte migration during inflammation, *Immunol. Res.* 22, 299–317.
2. Ley, K. (2003) The role of selectins in inflammation and disease, *Trends Mol. Med.* 9, 263–268.
3. Vestweber, D., and Blanks, J. E. (1999) Mechanisms that regulate the function of the selectins and their ligands, *Physiol. Rev.* 79, 181–213.

4. Alon, R., Hammer, D. A., and Springer, T. A. (1995) Lifetime of the P-selectin-carbohydrate bond and its response to tensile force in hydrodynamic flow, *Nature* 374, 539–542.
5. Kaplanski, G., Farnarier, C., Tissot, O., Pierres, A., Benoliel, A. M., Alessi, M. C., Kaplanski, S., and Bongrand, P. (1993) Granulocyte-endothelium initial adhesion. Analysis of transient binding events mediated by E-selectin in a laminar shear flow, *Biophys. J.* 64, 1922–1933.
6. Marshall, B. T., Long, M., Piper, J. W., Yago, T., McEver, R. P., and Zhu, C. (2003) Direct observation of catch bonds involving cell-adhesion molecules, *Nature* 423, 190–193.
7. Sarangapani, K. K., Yago, T., Klopocki, A. G., Lawrence, M. B., Fieger, C. B., Rosen, S. D., McEver, R. P., and Zhu, C. (2004) Low force decelerates L-selectin dissociation from P-selectin glycoprotein ligand-1 and endoglycan, *J. Biol. Chem.* 279, 2291–2298.
8. Yago, T., Wu, J., Wey, C. D., Klopocki, A. G., Zhu, C., and McEver, R. P. (2004) Catch bonds govern adhesion through L-selectin at threshold shear, *J. Cell Biol.* 166, 913–923.
9. Phan, U. T., Waldron, T. T., and Springer, T. A. (2006) Remodeling of the lectin-EGF-like domain interface in P- and L-selectin increases adhesiveness and shear resistance under hydrodynamic force, *Nat. Immunol.* 7, 883–889.
10. Lou, J., Yago, T., Klopocki, A. G., Mehta, P., Chen, W., Zarnitsyna, V. I., Bovin, N. V., Zhu, C., and McEver, R. P. (2006) Flow-enhanced adhesion regulated by a selectin interdomain hinge, *J. Cell Biol.* 174, 1107–1117.
11. Nicholson, M. W., Barclay, A. N., Singer, M. S., Rosen, S. D., and van der Merwe, P. A. (1998) Affinity and kinetic analysis of L-selectin (CD62L) binding to glycosylation-dependent cell-adhesion molecule-1, *J. Biol. Chem.* 273, 763–770.
12. McEver, R. P. (1997) Selectin-carbohydrate interactions during inflammation and metastasis, *Glycoconjugate J.* 14, 585–591.
13. Vanderslice, P., Biediger, R. J., Woodside, D. G., Berens, K. L., Holland, G. W., and Dixon, R. A. (2004) Development of cell adhesion molecule antagonists as therapeutics for asthma and COPD, *Pulm. Pharmacol. Ther.* 17, 1–10.
14. Ates, A., Kinikli, G., Turgay, M., and Duman, M. (2004) Serum-soluble selectin levels in patients with rheumatoid arthritis and systemic sclerosis, *Scand. J. Immunol.* 59, 315–320.
15. Blankenberg, S., Barbaux, S., and Tiret, L. (2003) Adhesion molecules and atherosclerosis, *Atherosclerosis* 170, 191–203.
16. Borsig, L. (2004) Selectins facilitate carcinoma metastasis and heparin can prevent them, *News Physiol. Sci.* 19, 16–21.
17. Phillips, M. L., Nudelman, E., Gaeta, F. C., Perez, M., Singhal, A. K., Hakomori, S., and Paulson, J. C. (1990) ELAM-1 mediates cell adhesion by recognition of a carbohydrate ligand, sialyl-Lex, *Science* 250, 1130–1132.
18. Norman, K. E., Anderson, G. P., Kolb, H. C., Ley, K., and Ernst, B. (1998) Sialyl Lewis(x) (sLe(x)) and an sLe(x) mimetic, CGP69669A, disrupt E-selectin-dependent leukocyte rolling in vivo, *Blood* 91, 475–483.
19. Tojo, S. J., Yokota, S., Koike, H., Schultz, J., Hamazume, Y., Misugi, E., Yamada, K., Hayashi, M., Paulson, J. C., and Morooka, S. (1996) Reduction of rat myocardial ischemia and reperfusion injury by sialyl Lewis x oligosaccharide and anti-rat P-selectin antibodies, *Glycobiology* 6, 463–469.
20. Buerke, M., Weyrich, A. S., Zheng, Z., Gaeta, F. C., Forrest, M. J., and Lefer, A. M. (1994) Sialyl Lewisx-containing oligosaccharide attenuates myocardial reperfusion injury in cats, *J. Clin. Invest.* 93, 1140–1148.
21. Ohnishi, M., Imanishi, N., and Tojo, S. J. (1999) Protective effect of anti-P-selectin monoclonal antibody in lipopolysaccharide-induced lung hemorrhage, *Inflammation* 23, 461–469.
22. Jacob, G. S., Kirmaier, C., Abbas, S. Z., Howard, S. C., Steininger, C. N., Welply, J. K., and Scudder, P. (1995) Binding of sialyl Lewis x to E-selectin as measured by fluorescence polarization, *Biochemistry* 34, 1210–1217.
23. Bendas, G. (2005) Inhibitors of membrane receptors involved with leukocyte extravasation, *Mini-Rev. Med. Chem.* 5, 575–584.
24. Beauharnois, M. E., Lindquist, K. C., Marathe, D., Vanderslice, P., Xia, J., Matta, K. L., and Neelamegham, S. (2005) Affinity and kinetics of sialyl Lewis-X and core-2 based oligosaccharides binding to L- and P-selectin, *Biochemistry* 44, 9507–9519.
25. Somers, W. S., Tang, J., Shaw, G. D., and Camphausen, R. T. (2000) Insights into the molecular basis of leukocyte tethering and rolling revealed by structures of P- and E-selectin bound to sLe(x) and PSGL-1, *Cell* 103, 467–479.
26. Skinner, M. P., Fournier, D. J., Andrews, R. K., Gorman, J. J., Chesterman, C. N., and Berndt, M. C. (1989) Characterization of human platelet GMP-140 as a heparin-binding protein, *Biochem. Biophys. Res. Commun.* 164, 1373–1379.
27. Skinner, M. P., Lucas, C. M., Burns, G. F., Chesterman, C. N., and Berndt, M. C. (1991) GMP-140 binding to neutrophils is inhibited by sulfated glycans, *J. Biol. Chem.* 266, 5371–5374.
28. Ludwig, R. J., Boehme, B., Podda, M., Henschler, R., Jager, E., Tandi, C., Boehncke, W. H., Zollner, T. M., Kaufmann, R., and Gille, J. (2004) Endothelial P-selectin as a target of heparin action in experimental melanoma lung metastasis, *Cancer Res.* 64, 2743–2750.
29. Nelson, R. M., Cecconi, O., Roberts, W. G., Aruffo, A., Linhardt, R. J., and Bevilacqua, M. P. (1993) Heparin oligosaccharides bind L- and P-selectin and inhibit acute inflammation, *Blood* 82, 3253–3258.
30. Koenig, A., Norgard-Sumnicht, K., Linhardt, R., and Varki, A. (1998) Differential interactions of heparin and heparan sulfate glycosaminoglycans with the selectins. Implications for the use of unfractionated and low molecular weight heparins as therapeutic agents, *J. Clin. Invest.* 101, 877–889.
31. Xie, X., Rivier, A. S., Zakrzewicz, A., Bernimoulin, M., Zeng, X. L., Wessel, H. P., Schapira, M., and Spertini, O. (2000) Inhibition of selectin-mediated cell adhesion and prevention of acute inflammation by nonanticoagulant sulfated saccharides. Studies with carboxyl-reduced and sulfated heparin and with trestatin a sulfate, *J. Biol. Chem.* 275, 34818–34825.
32. Gao, Y., Li, N., Fei, R., Chen, Z., Zheng, S., and Zeng, X. (2005) P-Selectin-mediated acute inflammation can be blocked by chemically modified heparin, RO-heparin, *Mol. Cells* 19, 350–355.
33. Wang, L., Brown, J. R., Varki, A., and Esko, J. D. (2002) Heparin's anti-inflammatory effects require glucosamine 6-O-sulfation and are mediated by blockade of L- and P-selectins, *J. Clin. Invest.* 110, 127–136.
34. Wei, M., Tai, G., Gao, Y., Li, N., Huang, B., Zhou, Y., Hao, S., and Zeng, X. (2004) Modified heparin inhibits P-selectin-mediated cell adhesion of human colon carcinoma cells to immobilized platelets under dynamic flow conditions, *J. Biol. Chem.* 279, 29202–29210.
35. Hopfner, M., Alban, S., Schumacher, G., Rothe, U., and Bendas, G. (2003) Selectin-blocking semisynthetic sulfated polysaccharides as promising anti-inflammatory agents, *J. Pharm. Pharmacol.* 55, 697–706.
36. Fritzsche, J., Alban, S., Ludwig, R. J., Rubant, S., Boehncke, W. H., Schumacher, G., and Bendas, G. (2006) The influence of various structural parameters of semisynthetic sulfated polysaccharides on the P-selectin inhibitory capacity, *Biochem. Pharmacol.* 72, 474–485.
37. Wang, J. G., and Geng, J. G. (2003) Affinity and kinetics of P-selectin binding to heparin, *Thromb. Haemostasis* 90, 309–316.
38. Sauerbrey, G. (1959) Verwendung von Schwingquarzen zur Wägung dünner Schichten und zur Mikrowägung, *Z. Phys.* 155, 206–222.
39. Xu, H., and Schlenoff, J. B. (1994) Kinetics, isotherms and competition in polymer adsorption using the quartz crystal microbalance, *Langmuir* 10, 241–245.
40. Kurosawa, S., Aizawa, H., Miyake, J., Yoshimoto, M., Hilborn, J., and Talib, Z. A. (2002) Detection of deposition rate of plasma-polymerized silicon-containing films by quartz crystal microbalance, *Thin Solid Films* 407, 1–6.
41. Hoshino, Y., Kawasaki, T., and Okahata, Y. (2006) Effect of ultrasound on DNA polymerase reactions: monitoring on a 27-MHz quartz crystal microbalance, *Biomacromolecules* 7, 682–685.
42. Yvin, J., Alban, S., and Franz, G. Anti-inflammatory and healing medicine based on laminarin sulfate. PCT Int. Appl. Patent No WO 2002036132, May 2002.
43. Alban, S., and Franz, G. (2001) Partial synthetic glucan sulfates as potential new antithrombotics: a review, *Biomacromolecules* 2, 354–361.
44. Alban, S., and Franz, G. (1994) Gas-liquid chromatography-mass spectrometry analysis of anticoagulant active curdlan sulfates, *Semin. Thromb. Hemostasis* 20, 152–158.



45. Minunni, M., Mascini, M., Guilbault, G. G., and Hock, B. (1995) The quartz crystal microbalance as biosensor. A Status Report on its Future, *Anal. Lett.* 28, 749–764.
46. Mehta, P., Cummings, R. D., and McEver, R. P. (1998) Affinity and kinetic analysis of P-selectin binding to P-selectin glycoprotein ligand-1, *J. Biol. Chem.* 273, 32506–32513.
47. Ludwig, R. J., Alban, S., Bistran, R., Boehncke, W. H., Kaufmann, R., Henschler, R., and Gille, J. (2006) The ability of different forms of heparins to suppress P-selectin function in vitro correlates to their inhibitory capacity on bloodborne metastasis in vivo, *Thromb. Haemostasis* 95, 535–540.
48. Mousa, S. A. (2004) Heparin and low molecular weight heparin in thrombosis, cancer, and inflammatory diseases, *Methods Mol. Med.* 93, 35–48.

BI602347G